© 2014. Published by The Company of Biologists Ltd | Development (2014) 141, 3188-3196 doi:10.1242/dev.106690

RESEARCH ARTICLE

# Leading and trailing cells cooperate in collective migration of the zebrafish posterior lateral line primordium

**Damian Dalle Nogare[1], Katherine Somers[1], Swetha Rao[1], Miho Matsuda[1,2], Michal Reichman-Fried[3], Erez Raz[3] and Ajay B. Chitnis[1,*]**

## ABSTRACT

Collective migration of cells in the zebrafish posterior lateral line primordium (PLLp) along a path defined by Cxcl12a expression depends on Cxcr4b receptors in leading cells and on Cxcr7b in trailing cells. Cxcr7b-mediated degradation of Cxcl12a by trailing cells generates a local gradient of Cxcl12a that guides PLLp migration. Agent-based computer models were built to explore how a polarized response to Cxcl12a, mediated by Cxcr4b in leading cells and prevented by Cxcr7b in trailing cells, determines unidirectional migration of the PLLp. These chemokine signaling-based models effectively recapitulate many behaviors of the PLLp and provide potential explanations for the characteristic behaviors that emerge when the PLLp is severed by laser to generate leading and trailing fragments. As predicted by our models, the bilateral stretching of the leading fragment is lost when chemokine signaling is blocked in the PLLp. However, movement of the trailing fragment toward the leading cells, which was also thought to be chemokine dependent, persists. This suggested that a chemokine-independent mechanism, not accounted for in our models, is responsible for this behavior. Further investigation of trailing cell behavior shows that their movement toward leading cells depends on FGF signaling and it can be re-oriented by exogenous FGF sources. Together, our observations reveal the simple yet elegant manner in which leading and trailing cells coordinate migration; while leading cells steer PLLp migration by following chemokine cues, cells further back play follow-the-leader as they migrate toward FGFs produced by leading cells.

**KEY WORDS: FGF, Agent-based modeling, Chemokines, Collective migration, Lateral line, Zebrafish**

## INTRODUCTION

The lateral line is a sensory system in fish and amphibians, which detects water flow over the surface of the animal. It consists of sensory organs called neuromasts arrayed in a stereotyped pattern over the body. Each neuromast contains sensory hair cells at its center, tuned to detect water flow in a particular direction. Establishment of the posterior lateral line system in zebrafish is pioneered during the second day of development by the posterior lateral line primordium (PLLp), a cluster of ~125 cells that forms near the otic vesicle. From its position caudal to the otic vesicle, the cell cohort of the PLLp migrates collectively along the horizontal myoseptum to the tip of the tail, periodically depositing neuromasts, sequentially referred to as the L1, L2, L3, etc. neuromasts (Fig. 1A) (Gompel et al., 2001).

The PLLp in the zebrafish, *Danio rerio*, has emerged as an extraordinary model system in which to study collective cell migration, a type of migration broadly observed in a variety of developmental and disease contexts, including gastrulation, branching morphogenesis, epithelial wound healing and tissue repair, and invasive growth of tumor strands (for a review, see Friedl and Gilmour, 2009). During collective migration, direction-sensing and migratory behavior must be coordinated between many cells, while maintaining cohesive interactions. How this is achieved in various contexts is now only beginning to be understood. Chemokine signaling in the PLLp guides leading cells (David et al., 2002; Haas and Gilmour, 2006; Li et al., 2004); however, questions remain as to how exactly this system determines directional migration and how trailing cells follow leading cells of the PLLp.

Establishment of polarized Wnt and FGF signaling systems coordinates many aspects of morphogenesis, migration and cell fate specification in the PLLp (Fig. 1C; supplementary material Fig. S1A-E). Formation of nascent neuromasts or 'protoneuromasts' in the migrating PLLp is initiated by Wnt signaling-dependent secretion of FGFs by leading cells. However, Wnt signaling also induces expression of intracellular inhibitors of FGF receptor signaling such as Sef and Mkp3 (Aman and Piotrowski, 2008; Matsuda et al., 2013). So the FGFs, secreted in response to Wnt signaling in leading cells, are unable to activate FGF receptor signaling and sustain FGF receptor expression in these cells. Instead, the FGFs are delivered to an adjacent trailing domain, where activation of FGF receptors initiates protoneuromast formation and maintains FGF receptor expression. As additional protoneuromasts periodically form toward the leading end, previously formed protoneuromasts mature and are eventually deposited from the trailing end by the migrating primordium (Aman and Piotrowski, 2008; Nechiporuk and Raible, 2008).

The PLLp is guided along the horizontal myoseptum by the transient expression of the chemokine Cxcl12a (also known as Sdf1a) (David et al., 2002; Li et al., 2004). Directionality of PLLp migration is not encoded by graded expression of this chemoattractant signal, instead, directional migration requires the differential expression of two chemokine receptors, Cxcr4b and Cxcr7b (Dambly-Chaudiere et al., 2007; Valentin et al., 2007; Fig. 1B; supplementary material Fig. S1F,G). *cxcr4b* transcripts are most prominent in a leading domain, whereas *cxcr7b* transcripts are restricted to a trailing domain. However, there is a significant overlap between these two expression domains, and in reality

[1]Section on Neural Developmental Dynamics, Program in Genomics of Differentiation, Eunice Kennedy Shriver National Institute of Child Health and Human Development, National Institutes of Health, Bethesda, MD 20892-2790, USA. [2]Department of Cell Biology and Molecular Medicine, Rutgers, The State University of New Jersey, New Jersey Medical School, Newark, NJ 17101-1709, USA. [3]Institute of Cell Biology, Center for Molecular Biology of Inflammation, 48149 Münster, Germany.

*Author for correspondence (chitnisa@mail.nih.gov)

**Received 3 December 2013; Accepted 15 June 2014**

Development (2014) 141, 3188-3196 doi:10.1242/dev.106690

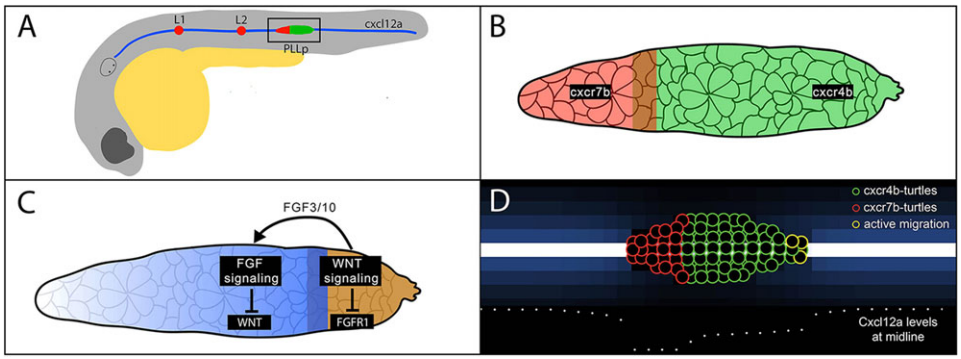


**Fig. 1. Schematic of PLLp migration, gene expression domains and example model output.** (A) Schematic of PLLp migration along the myoseptum. (B) Detail of the region outlined in A, showing approximate expression domains of *cxcr4b* and *cxcr7b*. (C) Schematic of juxtaposed Wnt and FGF signaling domains in the PLLp. Arrow indicates diffusion of FGF3 and FGF10A. (D) Example of PLLp computational model. In all model figures green circles represent *cxcr4b-turtles*, red circles represent *cxcr7b-turtles* and yellow circles represent actively migrating *turtles*. Blue shades show levels of Cxcl12a in *patches*.

Cxcr4b protein is distributed throughout the PLLp, including the trailing domain (Dona et al., 2013).

Several models for how these receptors impart directional movement to the PLLp have been proposed based on either differences in their ability to allow cells to respond to chemokines with migratory behavior or in their role in facilitating internalization and subsequent degradation of the chemokines. One model suggests that whereas Cxcr4b is capable of binding Cxcl12a and triggering migratory behavior, Cxcr7b is not. Instead, it promotes the rapid internalization and degradation of Cxcl12a (Burns et al., 2006; Boldajipour et al., 2008; Naumann et al., 2010). In the context of the PLLp, this hypothesis implies that Cxcr7b in the trailing domain locally depletes the chemokine, thus creating a gradient of chemokine availability along the length of the PLLp (Dambly-Chaudiere et al., 2007; Ghysen and Dambly-Chaudiere, 2007). This, it has been suggested, ensures that Cxcr4b-expressing cells steer migration by responding to the relatively high levels of chemokine they see at the leading end of the PLLp. Another model suggests that if all the PLLp cells were to internalize and degrade Cxcl12a, then, as the PLLp migrates, it would degrade Cxcl12a in its path, leaving less in its wake. The resulting asymmetry in the distribution of Cxcl12a, this model suggests, could also account for directed PLLp migration (Streichan et al., 2011).

Recent studies have directly examined the Cxcl12a gradient during primordium migration (Dona et al., 2013; Venkiteswaran et al., 2013). For example, using tools that measure the lifetime of the Cxcr4b receptor, Dona et al. infer the presence of a gradient of Cxcr4b internalization along the length of the PLLp by demonstrating a shorter receptor lifetime in leading cells compared with trailing cells. Internalization of Cxcr4b is determined by its interaction with Cxcl12a. The average lifetime of the Cxcr4b receptor in this study has therefore been interpreted to reflect a gradient in the availability of Cxcl12a in the surrounding environment. These data support a model by which trailing cells act as a sink to polarize Cxcl12a availability to Cxcr4b along the length of the PLLp. However, these studies leave important questions unanswered: is the primary purpose of Cxcl12a internalization by Cxcr7b in trailing cells to provide directional information via a chemokine gradient to leading cells in order to polarize their migration; or is the primary function of ligand degradation by Cxcr7b to prevent Cxcr4b activation in trailing cells?

Evidence from transplant experiments shows that even a small number of transplanted wild-type cells can rescue Cxcl12a-mediated migration in a *cxcr4b* mutant PLLp. However, they appear to do so only when positioned at the leading edge of the PLLp (Valentin et al., 2007). This suggests that Cxcr4b is essential only in cells that are at the leading end of the PLLp and that Cxcr4b-mediated chemokine signaling may operate to determine a migratory response only when Cxcr4b-expressing cells are at one or more edges of the PLLp. On the other hand, when transplanted *cxcr4b* mutant cells are not at the leading end of a wild-type PLLp and are in the interior of the PLLp, they are able to migrate and behave indistinguishably from their wild-type counterparts (Haas and Gilmour, 2006). This suggests that movement of trailing cells in the PLLp does not require Cxcr4b-mediated chemokine signaling and that alternate mechanisms govern collective migration of trailing cells within the PLLp.

In the present study, agent-based computational models were built to explore how a migratory response to Cxcl12a, which is mediated by Cxcr4b in leading cells, could determine unidirectional migration of the PLLp when coupled with local depletion of Cxcl12a by chemokine receptors. The models were able to recapitulate PLLp behavior in a variety of situations. We describe experimental manipulations of the PLLp designed to test some of the predictions of the chemokine signaling-based model of PLLp migration. Analysis of these experiments now suggests that the primary role of Cxcr7b-mediated degradation by trailing cells is to ensure a polarized response to Cxcl12a by ensuring Cxcr4b receptors in trailing cells do not have access to the chemokine.

Although our chemokine signaling-based models were able to account for various behaviors of leading cells, they could not account for specific chemokine-independent behaviors of trailing cells in the PLLp. Further experimental investigation of trailing cell behavior in this study now reveals the simple yet elegant manner in which leading and trailing cells coordinate their migration. We show that while leading cells steer PLLp migration by following chemokine cues, trailing cells play follow-the-leader as they migrate toward FGFs produced by leading cells. Our study illustrates how the development of an agent-based model has allowed us to visualize how chemokine signaling determines collective migration of the PLLp and to account for some complex emergent behaviors of the PLLp. More importantly, however, the study illustrates how the failure of the model to recapitulate specific behaviors has played a key role in inspiring a series of experiments that now provide a more-integrated view of how leading and trailing cells cooperate to guide collective migration of the PLLp.

## RESULTS

### Construction of an agent-based model of PLLp migration

We constructed agent-based computational models of the PLLp in the modeling environment Netlogo (Wilensky, 1999) to explore the potential roles of leading Cxcr4b- and trailing Cxcr7b-expressing cells in degrading Cxcl12a and guiding migration of the PLLp. This programming environment consists of individual mobile agents called *turtles*, where multiple *breeds* of *turtles* can be defined that behave according to distinct sets of rules. In addition there are *links* that form visco-elastic connections between defined sets of *turtles*

Development (2014) 141, 3188-3196 doi:10.1242/dev.106690

and individual non-motile agents called *patches*, which define the environment in which the *turtles* operate.

In our models, *patches* are used to represent the substrate upon which the PLLp migrates and to define the source of Cxcl12a. *Patches* in a horizontal stripe one-cell wide along the middle of our model world, representing the horizontal myoseptum, produce Cxcl12a (Fig. 1D). It diffuses and is degraded at a defined rate by the *patches*. The PLLp is made of two *breeds* of *turtles* (Fig. 1D): a leading compartment of *Cxcr4-turtles* (green), representing cells that only express Cxcr4b; and a trailing compartment of *Cxcr7b-turtles* (red) that represent cells expressing both Cxcr4b and Cxcr7b. As transplant experiments suggest that only cells at the edges of the PLLp move in response to Cxcl12a in their environment, we replicate this in the model so that only *turtles* at a free edge respond to Cxcl12a.

*Links* connect adjacent *turtles* and model adhesive interactions between cells of the PLLp. Although movement of the PLLp is initiated by the movement of *turtles* at the edge of the PLLp, the visco-elastic *links* indirectly determine the movement of the remaining cells of the model PLLp. This implementation assumes that coordinated movement of cells within the PLLp is determined by the adhesive or mechanical coupling of cells. Though this simplification ignores additional mechanisms that determine active migration of trailing cells, it allowed us to focus on chemokine-dependent migratory behavior in these models. The model file (pLLP model.zip) and details on its construction can be found in the supplementary material. Readers are encouraged to experiment with the model using the Netlogo software, available at http://ccl.northwestern.edu/netlogo/.

### The absolute level, rather than a gradient of Cxcl12a, determines the migratory response

During the construction of agent-based models, we had to decide whether some minimal gradient or some threshold level of Cxcl12a determines migratory behavior of *Cxcr4b-turtles* in the PLLp. To test which of these determines protrusive cell behavior in the actual PLLp, we used heatshock to induce broad ectopic expression of Cxcl12a in *Tg(hsp:cxcl12a)* embryos (Knaut et al., 2005). Broad ectopic expression was expected to increase the absolute level of Cxcl12a, while at the same time flatten the endogenous gradient (Dona et al., 2013). Protrusive activity was no longer primarily observed at the leading end of the PLLp following heatshock-induced Cxcl12a expression; instead, protrusive activity was seen around the entire edge of a leading domain of the PLLp, where *cxcr7b* was not expressed (Fig. 2A-D; supplementary material Movie 1 and Fig. S2). This suggested that protrusive activity is determined by the level of Cxcl12a present, rather than by the steepness of the Cxcl12a gradient. However, protrusive activity remained low in the trailing area, where *cxcr7b* is expressed (Fig. 2B,D). This suggested that, despite relatively high levels of induced expression, Cxcr7b-expressing cells prevent Cxcr4b receptors in trailing cells from having access to levels of Cxcl12a that are high enough to stimulate chemokine-dependent protrusive activity.

Based on these observations, we implemented migratory behavior in our models that was determined by the absolute level of Cxcl12a encountered by the *cxcr4b-turtles*, rather than the steepness of the Cxcl12a gradient. Specifically, at each time step, each *cxcr4b-turtle* orients in a random direction, checks that there is no *turtle* ahead (confirming it is an edge of the PLLp), and then, if the absolute level of Cxcl12a in the empty *patch* ahead exceeds some defined threshold, it moves ahead (see model description in the supplementary material for details). In our models, the green *cxcr4b-turtles* undergoing this migratory response to Cxcl12a transiently assume a yellow color so their 'protrusive' activity can be monitored in simulations.

We also assumed relatively high levels of Cxcl12a degradation by trailing *cxcr7b-turtles*. This prevented trailing cells from being exposed to levels of Cxcl12a that exceed the threshold required to determine a migratory response, even in the context of broad exaggerated Cxcl12a expression. Simulations incorporating these parameters illustrate how protrusive activity in the model PLLp, represented by the migratory response of individual *turtles*, recapitulates what is seen in the actual PLLp, both in control embryos and in embryos with heatshock-induced Cxcl12a expression (Fig. 2G-K, compare with D). By contrast, when the migratory response was determined by the steepness of the Cxcl12a gradient, heatshock-induced Cxcl12a expression flattened the gradient and this was accompanied by reduced protrusive activity around the edges of the model PLLp, not increased protrusive activity as in the actual PLLp (Fig. 2I,L).

It was initially surprising to observe that, when high levels of Cxcl12a expression are induced with heatshock, trailing *cxcr7b*-expressing cells remain relatively unresponsive. However, 4 h after heatshock induction of *cxcl12a* expression there was a significant increase in *cxcr7b* transcript expression, which nevertheless remained confined to a trailing domain of the PLLp (Fig. 2E,F; quantified in supplementary material Fig. S3). This suggests that autoregulation of *cxcr7b* expression by Cxcl12a is part of a robust mechanism that ensures Cxcr4b receptors in trailing cells are not exposed to high levels of Cxcl12a.

### Chemokine-dependent models recapitulate the results of laser-dissection of the PLLp

Simulations of PLLp migration with models based on the assumptions described above were able to recapitulate directed migration (supplementary material Movie 2). To challenge our models, we asked how effectively they were able to recapitulate the behavior of the PLLp following experimental manipulations in which the PLLp was cut into individual fragments. The first such manipulation was based on an experiment initially described by Gilmour et al. (2009). In it, laser ablation of PLLp cells, just in front of the leading protoneuromast, was used to create two fragments: a small leading fragment with 10-20 cells, shown to contain only *cxcr4b*-expressing cells; and a larger trailing fragment, containing both leading *cxcr4b*- and trailing *cxcr7b*-expressing cells (supplementary material Fig. S4). The purpose of this experiment was to determine whether degradation of Cxcl12a by trailing PLLp cells creates a broad enough local depression in Cxcl12a availability to polarize migration of the leading *cxcr4b*-expressing fragment.

The outcome of this manipulation *in vivo* is complex and the two PLLp fragments display variable but reproducible behaviors following the laser cut. In most cases, the leading fragment moves forward a short distance and then stalls (Fig. 3A; supplementary material Movie 3). The stalling of the leading fragment suggests that clearance of Cxcl12a by trailing Cxcr7b-expressing cells is not adequate to maintain polarized caudal migration of the leading fragment, at least over long distances. Stalling of the leading fragment is accompanied by protrusive activity in both directions and stretching of the leading fragment (arrowheads in Fig. 3A). This stretching behavior is independent of the influence of the trailing fragment and was also observed when we performed an additional ablation wherein all trailing cells were removed (Fig. 3C). In this

Development (2014) 141, 3188-3196 doi:10.1242/dev.106690

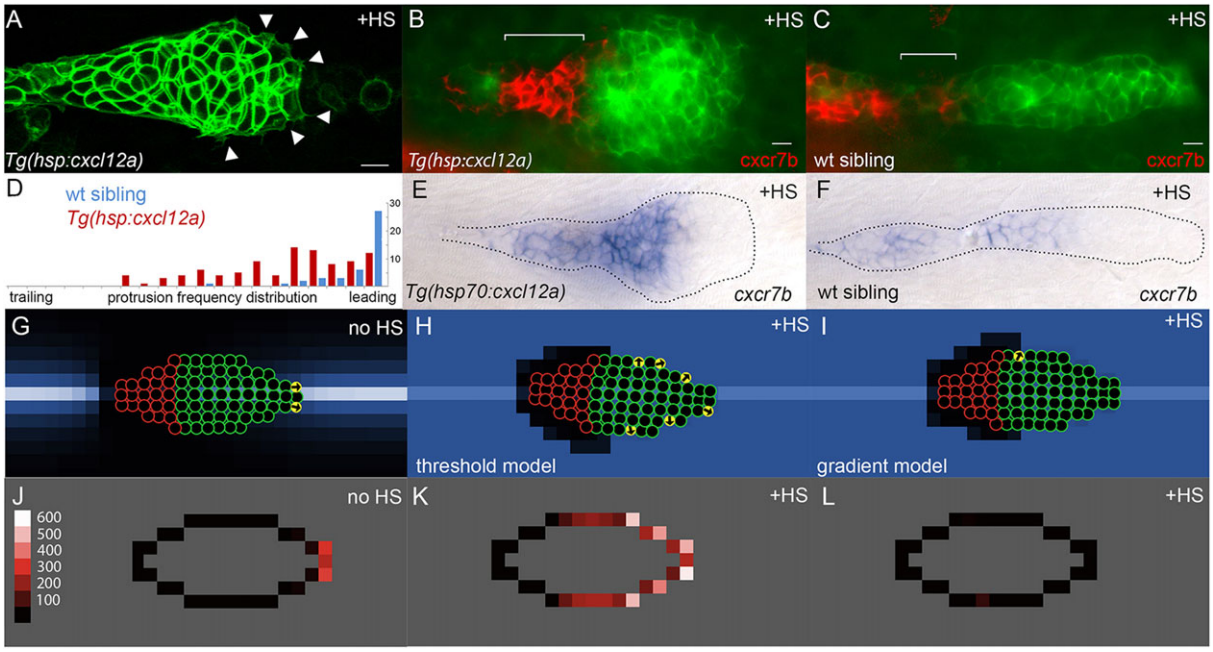


**Fig. 2. Experimental and simulated overexpression of Cxcl12a.** (A) Morphology of PLLp in *Tg(hsp:cxcl12a)* after 1 h of heatshock (corresponding to t=78 min in supplementary material Movie 1). Arrowheads indicate protrusions. (B,C) False-color overlay of *cxcr7b in situ* hybridization (red) in *Tg(hsp70:cxcl12a)* (B) and wild-type sibling embryo (C) after heatshock for 1 h and recovery for 2 h. (D) Frequency of protrusions observed from the leading to the trailing end of the PLLp in embryos with heatshock-induced *cxcl12a* expression (red bars, six embryos) compared with that in control siblings (blue, six embryos). Each bar represents the frequency of protrusions observed in 5% increments of the relative distance from the leading end of the PLLp observed. (E,F) *In situ* hybridization for *cxcr7b* transcript in *Tg(hsp:cxcl12a)* (E) and wild-type sibling (F) PLLp after a 30 min heatshock at 37.5°C and 4 h of recovery. (G) Model PLLp without heatshock. (H) Model PLLp after heatshock when *turtles* are migrating in response to above-threshold levels of Cxcl12a. (I) Model PLLp after heatshock when *turtles* are migrating in response to the gradient of Cxcl12a. (J-L) Time-averaged position of actively migrating *turtles* within model PLLp for the conditions in G-I, respectively. Scale ('protrusions'/1000 model iterations) is in J. Scale bars: 10 µm.

context, we observed the same stalling and bilateral stretching of the remaining leading fragment over the course of several (>7) hours of time-lapse imaging. In contrast to the stalling of the leading fragment, the polarized large trailing fragment initially stalls and then, following some delay, always resumes caudal migration (Fig. 3B). When the leading and trailing fragments come close enough to each other they eventually rejoin and the PLLp in its entirety resumes its migration (supplementary material Movie 3; Gilmour et al., 2009). When the gap between fragments is very short, no stalling is seen. Instead, the leading fragment continues to move forward, the trailing fragment follows, eventually catches up and joins, and the reconstituted PLLp resumes its caudal migration (data not shown).

Our agent-based model was able to easily reproduce many aspects of the behavior of both leading and trailing fragments (Fig. 3D; supplementary material Movie 4) and provided a potential explanation for it. The bi-directional stretching is consistent with the unpolarized *cxcr4b*-expressing leading fragment responding to

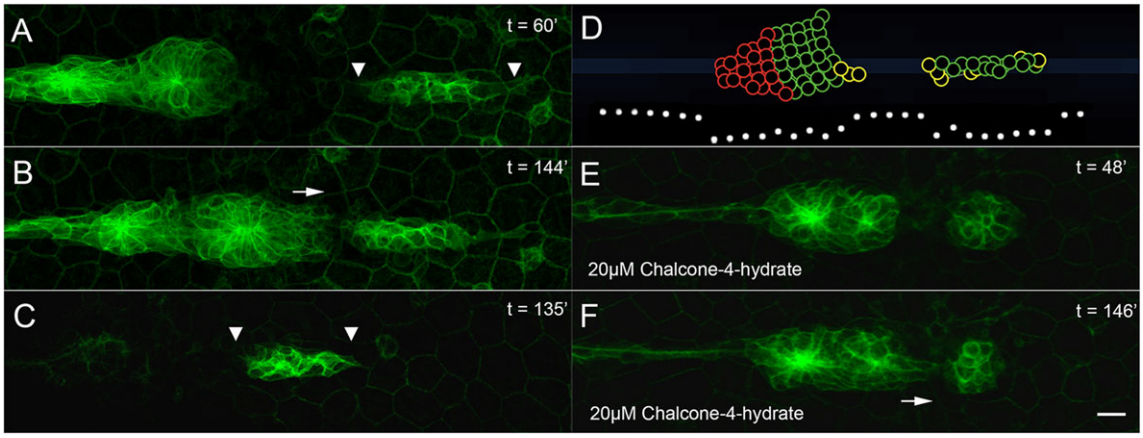


**Fig. 3. PLLp morphology following laser ablation.** (A) PLLp fragments 60 min after ablation to separate leading cells from trailing cells. Arrowheads indicate stretching of the leading fragment. (B) As in A, 144 min after ablation. Arrow indicates migration of trailing cells toward leading cells. (C) PLLp 135 min after complete ablation of trailing cells. Arrowheads indicate stretching of leading fragment. (D) Model ablation showing *cxcr4b* (green) and *cxcr7b* (red) *turtles*. White dots indicate the levels of Cxcl12a along the midline. (E) PLLp fragments 90 min after ablation in the presence of 20 µM chalcone-4-hydrate. Leading cells adopt a rounded morphology. (F) Same embryo as in E, 148 min after ablation. Arrow indicates migration of trailing cells toward leading cells. Scale bar: 10 µm.

Development (2014) 141, 3188-3196 doi:10.1242/dev.106690

chemokine cues at either end with protrusive activity. On the other hand, build up of newly secreted Cxcl12a between severed fragments could account for the movement of the trailing and leading fragments toward each other following their separation. These potential explanations suggested that both bilateral stretching of the leading fragment and the movement of the trailing fragment toward the leading fragment would be lost if responses to Cxcl12a were blocked.

To test these predictions, we repeated these experiments in the presence of chalcone-4-hydrate, an inhibitor of Cxcl12a activity (Hachet-Haas et al., 2008). We confirmed the efficacy of this inhibitor by first demonstrating that treatment with 10 µM of chalcone-4-hydrate resulted in slowing and eventual stalling of PLLp migration (data not shown). In PLLps severed to create leading and trailing fragments after treatment with chalcone-4-hydrate to inhibit Cxcl12a signaling, we failed to observe bilateral stretching of the leading fragment. Instead, it appeared as a compact cluster of cells [average circularity 0.72±0.09 for treated ($n$=13) and 0.43±0.13 for DMSO treated ($n$=5) leading fragments after ablation, $P$<0.001, Fig. 3E]. These data confirm that stretching of the leading fragment is due to a bilateral response to Cxcl12a by both ends of the *cxcr4b*-expressing leading fragment, as suggested by our model.

On the other hand, exposure to chalcone-4-hydrate did not prevent the caudal migration of the trailing fragment toward the leading fragment (Fig. 3F; supplementary material Movie 5, 10/13 embryos). The persistent movement of the trailing fragment toward the leading fragment in the presence of an inhibitor of chemokine signaling suggested that this behavior did not depend on the polarized response of the trailing fragment to Cxcl12a, but may instead be related to the influence of leading cells on the trailing fragment. This possibility was supported by the observation that in some cases the trailing fragment appeared to leap toward the leading fragment (supplementary material Movie 3, lower panel), a phenomenon that could not be accounted for by our chemokine-based migration models.

### Laser ablation reveals a role for leading cells in guiding trailing cell migration

To further explore how leading cells influence trailing cells, we selected embryos at a stage when the PLLp has three protoneuromasts and laser ablated a stripe of cells both rostral and caudal to the central protoneuromast, mechanically isolating this protoneuromast from the remaining leading and trailing cells of the PLLp (Fig. 4A,B). This separated the PLLp into a trailing, middle and leading fragment. When examined, only the trailing fragment had *cxcr7b* expression (data not shown). Despite having no obvious physical link to either trailing or leading cells, the isolated middle fragment consistently moved toward the leading fragment of the PLLp (Fig. 4A,B,N), allowing it to reconnect eventually with the leading fragment (four out of four embryos; supplementary material Movie 6, top panel). This behavior is consistent with the leading fragment being the source of chemoattractive cues for the isolated middle fragment. On the other hand, it is also consistent with Cxcr7b in the trailing fragment locally degrading Cxcl12a and decreasing the likelihood of migratory behavior of the middle fragment toward trailing cells. A third possibility is that it is related to some inherent polarity in cells of the middle fragment, which allows them to continue migration for a short distance in their original direction of migration. It is important to note that the severing of physical connections between leading and trailing cell populations in this experiment suggests that adhesive mechanical connections are not essential for leading cells to initiate directional migration of trailing cells in this context.

To test these three hypotheses, we re-examined the behavior of isolated middle fragments following complete ablation of the leading and/or trailing fragments. When both leading and trailing fragments were ablated, the isolated middle fragment lost its polarized caudal migratory behavior (12 out of 13 embryos, Fig. 4C,D,N; supplementary material Movie 6, second panel). This argues against any inherent polarity determining this behavior, and suggests that leading and/or trailing fragments provide directional cues to cells in the middle fragment.

When the leading fragment was ablated but the trailing fragment was left intact, we did not observe polarized caudal movement of the middle fragment (Fig. 4E,F,N; supplementary material Movie 6, third panel, four out of five embryos). As the trailing fragment has the bulk of the Cxcr7b-expressing cells, its failure to significantly polarize migratory behavior of the middle fragment when they are separated suggests that degradation of Cxcl12a by Cxcr7b-expressing cells is insufficient to polarize chemokine-dependent migration of the middle fragment, at a distance, on its own.

When the trailing fragment was ablated, leaving the leading fragment intact, the middle fragment consistently moved caudally toward the leading fragment, and the two fragments eventually rejoined (Fig. 4G,H,N; supplementary material Movie 6, bottom panel, five out of five embryos). We confirmed by RNA *in situ* hybridization that the ablation did not affect expression of *cxcl12a* in the underlying myoseptum (Fig. 4I). Furthermore, the directional migration was not due to polarized expression of *cxcr4b* and *cxcr7b* in the middle fragment (Fig. 4J,K). Together, these observations demonstrate that movement of the middle fragment toward the leading fragment is likely to be a response to attractive cues from the leading fragment.

### FGFs mediate attraction of trailing cells toward leading cells

What guidance cue might leading cells provide for trailing cells? As noted earlier, cells in the leading zone are a source of FGF ligands (Aman and Piotrowski, 2008). FGFs serve as migratory cues in a variety of other contexts (Kadam et al., 2012; Vitorino and Meyer, 2008), making them strong candidates for providing a chemoattractive cue for trailing cells. Previous work has already shown that cryptic lamellipodia in trailing cells of the intact PLLp are normally polarized toward the leading edge, and that this polarization is lost upon inhibition of FGF signaling by treatment with the Fgfr1 inhibitor SU5402 (Lecaudey et al., 2008; Sun et al., 1999). It has also been shown that at an early stage of PLLp formation, around 18 hpf, isolated leading primordial cells are attracted toward the trailing PLLp cells by FGF signals (Breau et al., 2012). We determined by *in situ* hybridization that *fgf10a* expression is maintained in leading cells after ablation (Fig. 4L) and, furthermore, that *fgfr1* expression was restricted to trailing cells, as in the intact PLLp (Fig. 4M).

To test whether FGFs secreted by the leading cells are providing a chemoattractive cue for trailing cells during migration we first asked whether inhibition of FGF signaling prevents cells in a middle fragment from migrating toward the leading fragment. We pre-treated embryos with SU5402 for 2-4 h and then performed laser ablation to isolate a middle fragment of the PLLp. The trailing fragment was then ablated, leaving the middle and leading fragments intact. In the presence of SU5402 there was significantly less caudal movement of the middle fragment toward the leading fragment (Fig. 4N and Fig. 5A,B; supplementary material Movie 7, upper panel, $n$=9). However, in embryos in which SU5402 was washed out after ablation, we observed a gradual recovery of movement of the middle fragment toward the leading fragment and eventual joining of these two fragments in six out of seven embryos examined (Fig. 5C,D;

Development (2014) 141, 3188-3196 doi:10.1242/dev.106690

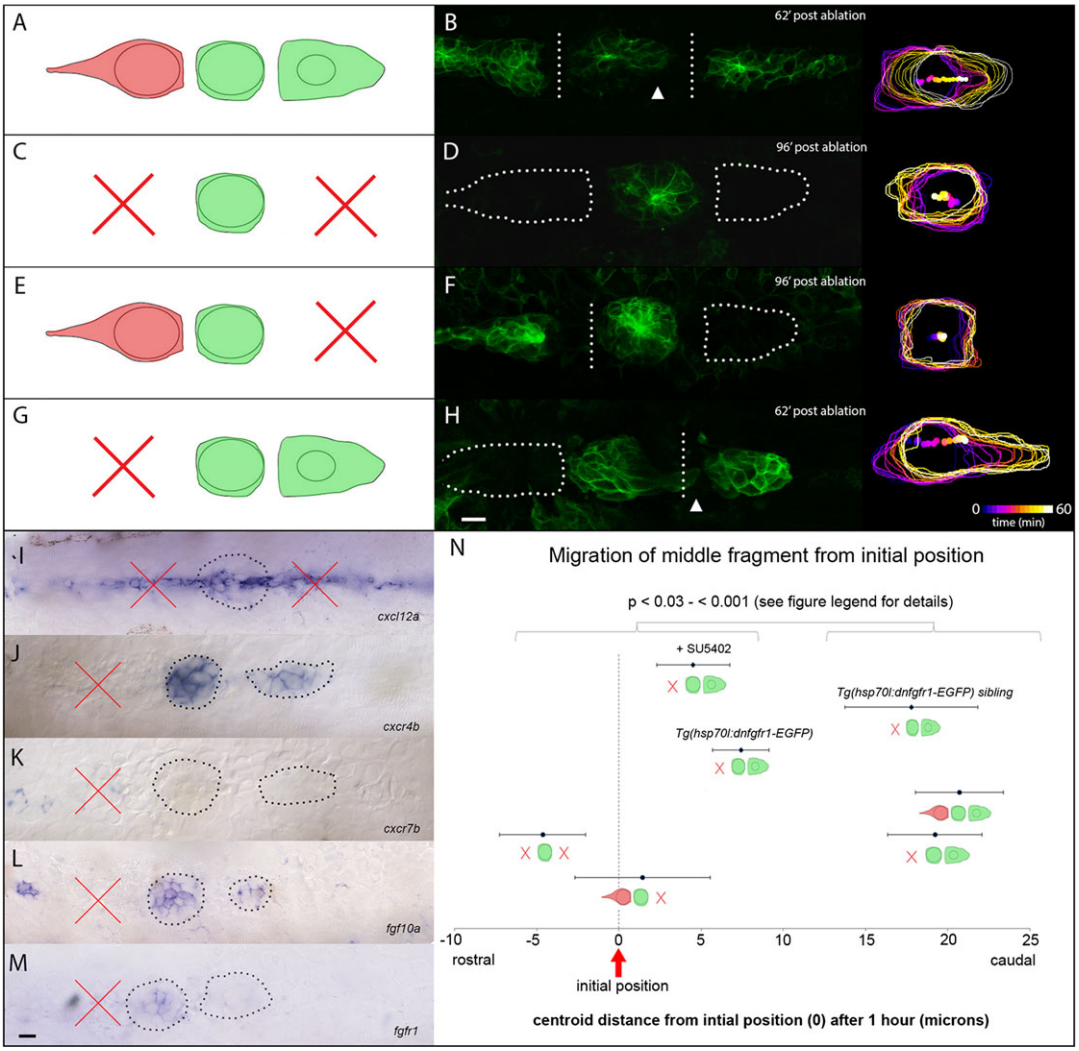


**Fig. 4. PLLp morphology following double laser ablation.** (A,B) Schematic of ablation and PLLp fragments 62 min after ablation to separate leading, middle and trailing fragments. Arrowhead indicates migration of middle fragment toward leading fragment. (C,D) Schematic of ablation and PLLp fragments 96 min after ablation to remove leading and trailing cells. (E,F) Schematic of ablation and PLLp fragments 96 min after ablation to separate middle from trailing cells, and remove leading cells. (G,H) Schematic of ablation and PLLp fragments 62 min after ablation to separate middle from leading cells, and remove trailing cells. Arrowhead indicates migration of trailing cells toward leading cells. Right panels in B,D,F,H show outlines and centroid position of middle fragments over time (see scale in H). (I) Expression of *cxcl12a* in the horizontal myoseptum after ablation. (J,K) Expression of *cxcr4b* (J) and *cxcr7b* (K) in PLLp immediately following ablation to generate isolated leading and middle fragments. (L,M) Expression of *fgf10a* (L) and *fgfr1* (M) in PLLp immediately following ablation to generate isolated leading and middle fragments. In I-M, dashed lines indicate PLLp fragments. Crosses indicate ablated fragments. (N) Quantification of middle fragment centroid movement in all experimental conditions, as indicated by diagrams (mean±s.e.m.). Statistical significances of all pairwise comparisons between the indicated groups fall between $P<0.03$ and $P<0.001$, Student's *t*-test. See supplementary material Table S2 for all pairwise statistical comparisons. Scale bars: 10 µm.

supplementary material Movie 7, lower panel). Similarly, in transgenic *Tg(hsp70l:dn-fgfr1)* embryos subjected to a 1 h heatshock, movement toward leading cells was also significantly inhibited compared with non-transgenic control sibling embryos (data not shown, quantification in Fig. 4N).

To demonstrate more directly that FGF can act as a chemotactic signal, we repeated the experiments with an isolated middle fragment to see whether the FGF-soaked beads could elicit the same polarized chemoattractive response from cells in the middle fragment that we had previously demonstrated could be elicited by the leading fragment. We again used laser ablation to isolate a middle fragment and then eliminated the remaining leading and trailing cells of the PLLp. After this ablation, we transplanted beads soaked in either FGF3 or BSA on opposing sides of the fragment and recorded the subsequent behavior of the cells by time-lapse microscopy (Fig. 6A,B). While the BSA-soaked bead provided a control for the effects of FGF, placement of two beads, one rostral and one caudal to the middle fragment, ensured that biased movement of the middle fragment was not related to unilateral tissue damage incurred during placement of beads. When FGF beads were placed caudally to the isolated middle fragment it migrated in the caudal direction just as they do toward an isolated leading fragment (six out of six embryos; Fig. 6A,C,E; another example is shown in supplementary material Movie 8, upper panel). Furthermore, when the FGF-soaked bead was placed rostrally, where the trailing fragment would normally be located, the cells reversed direction to migrate back toward the rostrally placed FGF3-soaked bead (five out of six embryos, Fig. 6B, D,E; supplementary material Movie 8, lower panel). These data suggest that exogenous FGF signals are sufficient to polarize migration of cells in an isolated middle fragment.

Development (2014) 141, 3188-3196 doi:10.1242/dev.106690

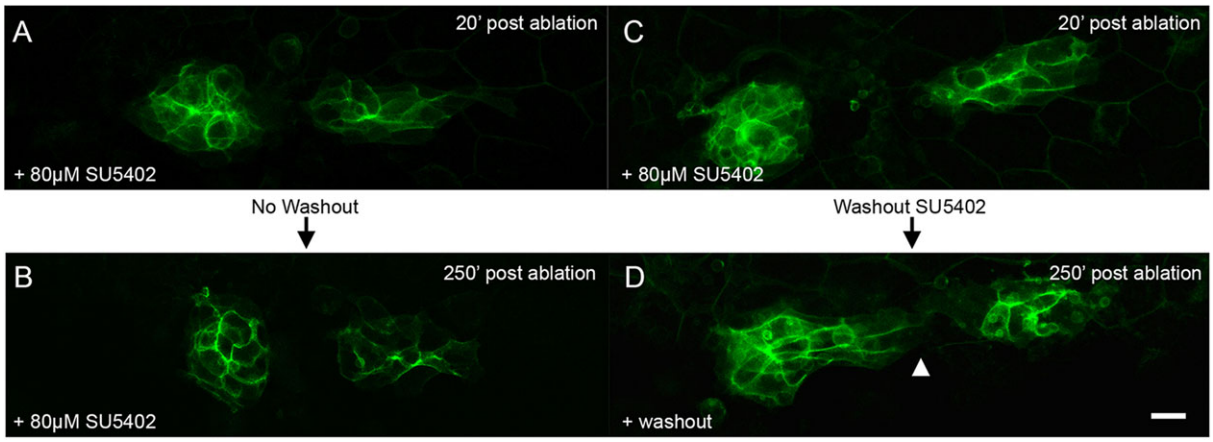


**Fig. 5. FGF signaling is required for polarized migration of the middle fragment.** (A,B) PLLp fragments 20 and 250 min after ablation, but in the presence of 80 μM SU5402. (C,D) PLLp fragment 20 and 250 min after ablation, with subsequent wash-out of SU5402. Arrowhead indicates migration of trailing cells toward leading cells. Scale bar: 10 μm.

## DISCUSSION

This study began with the development of an agent-based model of the PLLp to explore how polarized expression of the chemokine receptors, Cxcr4b and Cxcr7b, coupled with local depletion of the chemokine Cxcl12a by these receptors, determines directed collective migration of cells in the PLLp along a relatively uniform stripe of Cxcl12a expression. To test the agent-based model, we asked how well it recapitulates the behavior of a small leading and larger trailing fragment of the PLLp generated by laser ablation. As the agent-based model was able to recapitulate many of the observed *in vivo* behaviors of leading and trailing fragments, it was initially thought that their behaviors could be accounted for by the differential response of Cxcr4b and Cxcr7b receptors to dynamic changes in Cxcl12a expression. When this hypothesis was tested with a chemical inhibitor of Cxcl12a function, characteristic bilateral stretching of the leading fragment was lost. On the other hand, the movement of the trailing fragment toward the leading fragment persisted, suggesting that this behavior is independent of Cxcl12a-mediated chemokine signaling and that the leading fragment is a source of additional cues that determine polarized behavior of trailing cells. An investigation of this possibility revealed that FGFs produced by PLLp cells in a leading domain can influence the direction in which cells in more trailing domains migrate.

Previous studies have suggested Cxcr7b acts as a 'decoy' receptor by binding, internalizing and degrading Cxcl12a, rather than facilitating a protrusive migratory response to the chemokine. Other studies have shown that just a few Cxcr4b cells at the leading end or Cxcr7b cells at the trailing end are adequate to determine this polarized response of the PLLp (Valentin et al., 2007). However, our observations suggest it is unlikely that local degradation of Cxcl12a by trailing cells can establish a gradient that is broad enough to determine polarized migratory behavior of individual leading Cxcr4b-expressing cells at a distance. For example, a leading fragment of the PLLp generated by laser ablation, typically stretches bi-directionally in response to local Cxcl12a and does not maintain polarized caudal protrusions. Similarly, when laser ablation was used to generate a middle and trailing fragment, the trailing fragment, containing primarily Cxcr7b-expressing cells,

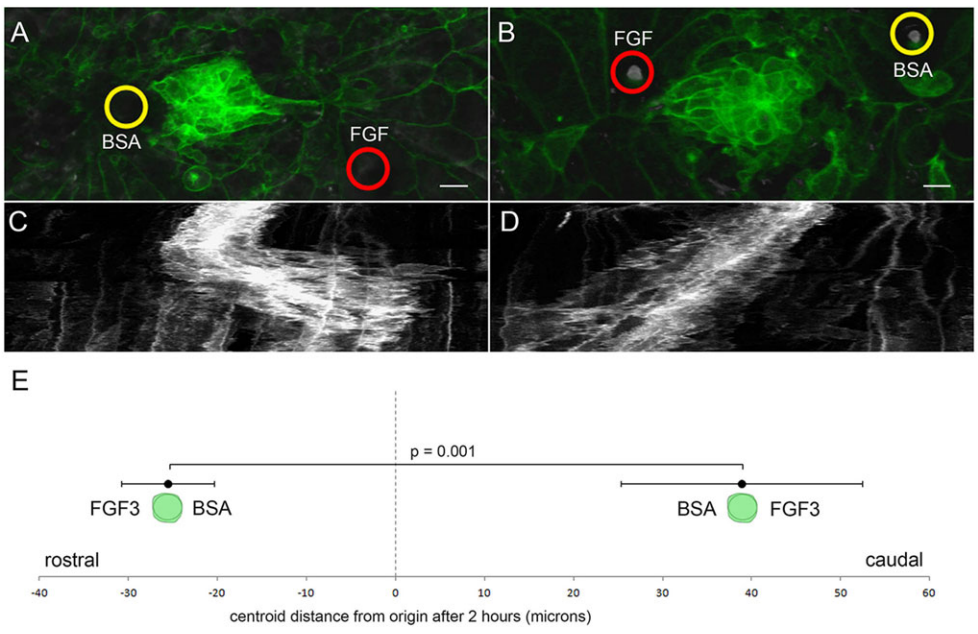


**Fig. 6. PLLp migration polarized by FGF-soaked beads.** (A) Morphology of the middle PLLp fragment after insertion of a FGF3-soaked (red circle) bead caudal to and a BSA soaked (yellow circle) bead rostral to the PLLp fragment. (B) Similar to A with position of the FGF3-soaked (red circle) and BSA-soaked (yellow circle) beads reversed. (C,D) Kymograph of cell behavior during a ~400 min time-lapse in A and B, respectively. (E) Quantification of movement of centroid position of cells (mean±s.e.m.) with FGF3-soaked beads either rostral or caudal to cells, as indicated. Scale bars: 10 μm.

Development (2014) 141, 3188-3196 doi:10.1242/dev.106690

was unable to deplete Cxcl12a in a manner that polarizes migration of the middle fragment.

Although local depletion by the Cxcr7b receptor may not be able to establish a Cxcl12a gradient that can influence migratory behavior of Cxcr4b-expressing cells at a distance, its local depletion by Cxcr7b receptors is likely to ensure that Cxcr4b receptors, also expressed in trailing cells, are unable respond to trailing Cxcl12a and determine migratory behavior in the opposite direction. Indeed our Cxcl12a heatshock experiments indicate that when cells are exposed to artificially high levels of Cxcl12a, this eventually induces higher levels of *cxcr7b* expression in trailing cells, ensuring the trailing domain with *cxcr7b* expression remains relatively unresponsive to the chemotactic influence of this chemokine.

If the primary role of Cxcr7b-dependent depletion of Cxcl12a is to prevent trailing Cxcr4b-expressing cells from responding to Cxcl12a, this could be achieved either by out competing Cxcr4b for binding to Cxcl12a, thereby reducing the available ligand, or by heterodimerizing with Cxcr4b to dampen downstream signaling (Levoye et al., 2009). A recent study has shown that Cxcr7b expressed exogenously in the lateral line nerve, which travels underneath the migrating PLLp, is able to non-autonomously rescue PLLp migration in a *cxcr7b* mutant (Dona et al., 2013). This supports the notion that lack of ligand availability to Cxcr4b may be adequate to prevent Cxcr4b activation in trailing cells. A predominantly local role for Cxcr7b in determining the response of trailing cells helps explain why restoring even a few Cxcr7b-expressing cells at the trailing end can restore directed migration of a *cxcr7b* mutant PLLp (Valentin et al., 2007).

We have described a chemoattractive role for FGF in polarizing the migration of trailing cells during collective migration of the lateral line primordium in zebrafish embryos. Previous studies showed that inhibition of FGF signaling by SU5402 results in loss of polarization of cryptic lamellipodia extended by trailing cells (Lecaudey et al., 2008). However, as these observations were made in an intact PLLp, they could be interpreted to suggest that FGF signaling orients processes extended by trailing cells based on a mechanism that requires transmission of mechanical tension from leading cells to trailing cells. As a severed leading fragment secreting FGFs or an ectopic source of FGFs can influence the migration of trailing cells, our study suggests FGF signaling organizes directed collective migration of trailing cells through a mechanism that can operate at a distance. However, this observation does not rule out an additional role for mechanical tension generated between in PLLp cells, determined by FGF signaling or other factors, in coordinating trailing cell migration, either within the intact PLLp or within the smaller fragments examined here. It is important to note that when the PLLp was severed to create a leading and middle fragment, *fgf10a* expression was seen in both middle and leading fragments, whereas *fgfr1* expression was absent in the leading fragment. Hence, it is not only the expression of FGFs by cells in the leading zone that determines polarized migration but also the polarized expression of the FGF receptor, the expression of which is significantly less in leading cells (supplementary material Fig. S1E; Fig. 4M). The mechanism by which FGF signals polarize migratory behavior remains unclear, as FGF does not simply promote protrusive migratory behavior. Rather, the presence of a sustained source of FGFs in the leading zone of the migrating PLLp appears to polarize migratory behavior in trailing cells that would otherwise be present but unpolarized in the absence of FGF signaling (Lecaudey et al., 2008).

Agent-based models provide a platform for understanding how similar behaviors emerge when cells interact by following specific rules, independent of the molecular pathways mediating these interactions. Similar strategies appear to be in operation during the collective migration of PLLp and neural crest cells. Long-range migration of cranial neural crest cells is determined by leading cells following VEGF cues secreted by the overlying ectoderm (McLennan et al., 2010). As with Cxcl12a in the lateral line system, leading crest cells do not follow an inherent VEGF concentration gradient, instead VEGF degradation by migrating neural crest cells ensures leading cells always encounter the highest levels of VEGF ahead in their path. However, depletion of VEGF prevents it from serving as an effective guidance cue for trailing cells, so trailing cells follow leading cells by a different strategy. Neural crest cells secrete a factor, C3a, which serves as a short-range chemoattractant (Carmona-Fontaine et al., 2011) that ensures crest cells migrate together. In this manner, though very different signaling systems are involved, collective migration in both the PLLp and neural crest systems involves a similar follow-the-leader strategy.

In the agent-based models described in this study, visco-elastic *links* between the *turtles* play a key role in determining collective migration. However, this aspect of the model is an over simplification. Though intercellular adhesions are likely to contribute in some way to collective migration in the PLLp, the trailing cells are not simply dragged along by leading cells. Instead, they actively migrate toward leading cells. Our experiments suggest that, in part, this is determined by the chemoattractive role of FGFs secreted by leading cells. However, the mechanisms that define cohesive migration in the PLLp remain poorly understood.

Future studies will determine how mechanical tension mediated by adhesion molecules, or by chemoattractants operating at short range, contribute to cohesive migration. The ideas discussed above will play a key role in the construction of the next generation of agent-based models of the PLLp. The iterative construction of such *in silico* models coupled with rigorous experimental validation promises a progressively deeper understanding of collective migration of the zebrafish PLLp system.

## MATERIALS AND METHODS

### Fish lines, chemical treatment and *in situ* hybridization

Zebrafish were maintained under standard conditions and staged according to Kimmel et al. (1995). All experiments used *Tg(clbnb:lynGFP)* transgenic embryos (Haas and Gilmour, 2006) generated by natural spawning. For heatshock induction of Cxcl12a expression, we used *Tg(hsp:cxcl12a)* embryos in a *Tg(clbnb:lynGFP)* background, heatshocked for 1 h at 37.5°C. For FGF receptor inhibition, embryos were treated with 20-80 µM SU5402 (Tocris) with shaking for 2-4 h prior to ablation. In practice, we observed significant manufacturer-to-manufacturer and batch-to-batch variability in the toxicity of SU5402, and as such each stock solution was independently titrated and concentrations between 20 and 80 µM were used. *Tg(hsp70l:dn-fgfr1)* (Lee et al., 2005) embryos were heatshocked for 1 h prior to ablation. For inhibition with chalcone-4-hydrate, embryos were placed in 10-20 µM inhibitor 30 min before ablation. *In situ* hybrization was performed as described elsewhere (Matsuda and Chitnis, 2010). To generate the false-color pictures in Fig. 2, *Tg(clbnb:lynGFP)* embryos were stained after *in situ* with anti-GFP antibody (Abcam). DIC images of NBT/BCIP *in situ* staining were inverted and false-colored in ImageJ (Schneider et al., 2012), then overlaid onto fluorescent images of anti-GFP staining.

### Laser ablation and time-lapse microscopy

To quantify protrusions following induction of *cxcl12a* expression, individual frames from time-lapse movies over ~3 h were examined and protrusions manually annotated. Protrusions were identified as dynamic membrane displacements, at least half a cell diameter in width, from the edge of the PLLp. The frequency of protrusions was measured based on the relative distance of each protrusion from the leading end of PLLp.

Development (2014) 141, 3188-3196 doi:10.1242/dev.106690

Laser ablation was performed either using a Mai-Tai DeepSee 2-photon laser at 800 nm on a Leica SP5 confocal microscope, or a 488 nm laser attached to a Zeiss Axioplan2 compound microscope. Embryos were anesthetized in 600 µM MS-222 (Sigma) and mounted in 0.8% low melting temperature agarose (NuSieve GTG) and placed in a solution of egg water with 600 µM tricaine for imaging. In most cases, the lateral line ganglion and part of the lateral line nerve adjacent to the otic vesicle was ablated before PLLp ablations were conducted. To standardize these manipulations as much as possible, we selected embryos between deposition of L1 and L3 neuromasts, at which time there are three protoneuromasts in the PLLp. We separated the PLLp into three fragments by ablating a ∼20 µm patch of cells on either side of the central protoneuromast within the migrating PLLp to create the isolated middle fragment. Time-lapse images were acquired on a Leica SP5 confocal microscope and images were processed using ImageJ and Fluorender (SCI Institute, http://www.sci.utah.edu/software/46-documentation/137-fluorender.html). Kymographs were made using ImageJ. Circularity was determined in ImageJ using the 'Circularity' measurement [circularity=$4\pi$ (area/perimeter$^2$)] on PLLp fragments. Centroid positions were determined in ImageJ by manual outlining of cell fragments.

### Bead transplantation and implantation

Approximately 50 µl of a suspension of 10 µm polystyrene beads (Polysciences) were rinsed twice in filter-sterilized PBS and pre-soaked in 0.5 mg/ml heparin solution for 20 min at room temperature. After removal of heparin, beads were incubated in 10 µl of either 0.1% BSA (for control beads) or 0.25 µg/µl recombinant FGF3 or FGF10 protein (R&D Systems) for 2 h at 16°C with shaking. Beads were implanted under the skin of ∼30-32 hpf embryos using a cell transplantation apparatus. For bilateral transplants, ablations were performed first, and then BSA- and FGF-soaked beads transplanted to either side of the remaining PLLp fragment.

#### Acknowledgements

We thank lab members for helpful comments, Chongmin Wang for fish care and Darren Gilmour for the ClaudinB-lyn GFP transgenic fish.

#### Competing interests

The authors declare no competing financial interests.

#### Author contributions

D.D.N. and A.B.C. conceived most of the experiments and wrote the manuscript. D.D.N. performed most of the experiments and developed models. K.S. helped with ablations, S.R. helped in coding models, M.M. performed some heatshock *cxcl12a* experiments with help from M.R.-F. and E.R.

#### Funding

The Intramural Program of the Eunice Kennedy Shriver National Institute of Child Health and Human Development (NICHD) and National Institutes of Health (NIH) [HD001012] supported this work. Deposited in PMC for release after 12 months.

#### Supplementary material

Supplementary material available online at
http://dev.biologists.org/lookup/suppl/doi:10.1242/dev.106690/-/DC1

#### References

**Aman, A. and Piotrowski, T.** (2008). Wnt/beta-catenin and Fgf signaling control collective cell migration by restricting chemokine receptor expression. *Dev. Cell* **15**, 749-761.

**Boldajipour, B., Mahabaleshwar, H., Kardash, E., Reichman-Fried, M., Blaser, H., Minina, S., Wilson, D., Xu, Q. and Raz, E.** (2008). Control of chemokine-guided cell migration by ligand sequestration. *Cell* **132**, 463-473.

**Breau, M. A., Wilson, D., Wilkinson, D. G. and Xu, Q.** (2012). Chemokine and Fgf signalling act as opposing guidance cues in formation of the lateral line primordium. *Development* **139**, 2246-2253.

**Burns, J. M., Summers, B. C., Wang, Y., Melikian, A., Berahovich, R., Miao, Z., Penfold, M. E. T., Sunshine, M. J., Littman, D. R., Kuo, C. J. et al.** (2006). A novel chemokine receptor for SDF-1 and I-TAC involved in cell survival, cell adhesion, and tumor development. *J. Exp. Med.* **203**, 2201-2213.

**Carmona-Fontaine, C., Theveneau, E., Tzekou, A., Tada, M., Woods, M., Page, K. M., Parsons, M., Lambris, J. D. and Mayor, R.** (2011). Complement fragment C3a controls mutual cell attraction during collective cell migration. *Dev. Cell* **21**, 1026-1037.

**Dambly-Chaudière, C., Cubedo, N. and Ghysen, A.** (2007). Control of cell migration in the development of the posterior lateral line: antagonistic interactions between the chemokine receptors CXCR4 and CXCR7/RDC1. *BMC Dev. Biol.* **7**, 23.

**David, N. B., Sapede, D., Saint-Etienne, L., Thisse, C., Thisse, B., Dambly-Chaudiere, C., Rosa, F. M. and Ghysen, A.** (2002). Molecular basis of cell migration in the fish lateral line: role of the chemokine receptor CXCR4 and of its ligand, SDF1. *Proc. Natl. Acad. Sci. USA* **99**, 16297-16302.

**Donà, E., Barry, J. D., Valentin, G., Quirin, C., Khmelinskii, A., Kunze, A., Durdu, S., Newton, L. R., Fernandez-Minan, A., Huber, W. et al.** (2013). Directional tissue migration through a self-generated chemokine gradient. *Nature* **503**, 285-289.

**Friedl, P. and Gilmour, D.** (2009). Collective cell migration in morphogenesis, regeneration and cancer. *Nat. Rev.* **10**, 445-457.

**Ghysen, A. and Dambly-Chaudiere, C.** (2007). The lateral line microcosmos. *Genes Dev.* **21**, 2118-2130.

**Gilmour, D., Haas, P., Lecaudey, V., Streichan, S. and Valentin, G.** (2009). S20-05 Dissecting the role of extrinsic and intrinsic cues in coordinating collective cell migration. *Mechanisms of Development.* **126**, Supplement, S21.

**Gompel, N., Cubedo, N., Thisse, C., Thisse, B., Dambly-Chaudière, C. and Ghysen, A.** (2001). Pattern formation in the lateral line of zebrafish. *Mech. Dev.* **105**, 69-77.

**Haas, P. and Gilmour, D.** (2006). Chemokine signaling mediates self-organizing tissue migration in the zebrafish lateral line. *Dev. Cell* **10**, 673-680.

**Hachet-Haas, M., Balabanian, K., Rohmer, F., Pons, F., Franchet, C., Lecat, S., Chow, K. Y. C., Dagher, R., Gizzi, P., Didier, B. et al.** (2008). Small neutralizing molecules to inhibit actions of the chemokine CXCL12. *J. Biol. Chem.* **283**, 23189-23199.

**Kadam, S., Ghosh, S. and Stathopoulos, A.** (2012). Synchronous and symmetric migration of Drosophila caudal visceral mesoderm cells requires dual input by two FGF ligands. *Development* **139**, 699-708.

**Kimmel, C. B., Ballard, W. W., Kimmel, S. R., Ullmann, B. and Schilling, T. F.** (1995). Stages of embryonic development of the zebrafish. *Dev. Dyn.* **203**, 253-310.

**Knaut, H., Blader, P., Strähle, U. and Schier, A. F.** (2005). Assembly of trigeminal sensory ganglia by chemokine signaling. *Neuron* **47**, 653-666.

**Lecaudey, V., Cakan-Akdogan, G., Norton, W. H. J. and Gilmour, D.** (2008). Dynamic Fgf signaling couples morphogenesis and migration in the zebrafish lateral line primordium. *Development* **135**, 2695-2705.

**Lee, Y., Grill, S., Sanchez, A., Murphy-Ryan, M. and Poss, K. D.** (2005). Fgf signaling instructs position-dependent growth rate during zebrafish fin regeneration. *Development* **132**, 5173-5183.

**Levoye, A., Balabanian, K., Baleux, F., Bachelerie, F. and Lagane, B.** (2009). CXCR7 heterodimerizes with CXCR4 and regulates CXCL12-mediated G protein signaling. *Blood* **113**, 6085-6093.

**Li, Q., Shirabe, K. and Kuwada, J. Y.** (2004). Chemokine signaling regulates sensory cell migration in zebrafish. *Dev. Biol.* **269**, 123-136.

**Matsuda, M. and Chitnis, A. B.** (2010). Atoh1a expression must be restricted by Notch signaling for effective morphogenesis of the posterior lateral line primordium in zebrafish. *Development* **137**, 3477-3487.

**Matsuda, M., Nogare, D. D., Somers, K., Martin, K., Wang, C. and Chitnis, A. B.** (2013). Lef1 regulates Dusp6 to influence neuromast formation and spacing in the zebrafish posterior lateral line primordium. *Development* **140**, 2387-2397.

**McLennan, R., Teddy, J. M., Kasemeier-Kulesa, J. C., Romine, M. H. and Kulesa, P. M.** (2010). Vascular endothelial growth factor (VEGF) regulates cranial neural crest migration in vivo. *Dev. Biol.* **339**, 114-125.

**Naumann, U., Cameroni, E., Pruenster, M., Mahabaleshwar, H., Raz, E., Zerwes, H.-G., Rot, A. and Thelen, M.** (2010). CXCR7 functions as a scavenger for CXCL12 and CXCL11. *PLoS ONE* **5**, e9175.

**Nechiporuk, A. and Raible, D. W.** (2008). FGF-dependent mechanosensory organ patterning in zebrafish. *Science* **320**, 1774-1777.

**Schneider, C. A., Rasband, W. S. and Eliceiri, K. W.** (2012). NIH Image to ImageJ: 25 years of image analysis. *Nat. Methods* **9**, 671-675.

**Streichan, S. J., Valentin, G., Gilmour, D. and Hufnagel, L.** (2011). Collective cell migration guided by dynamically maintained gradients. *Phys. Biol.* **8**, 045004.

**Sun, L., Tran, N., Liang, C., Tang, F., Rice, A., Schreck, R., Waltz, K., Shawver, L. K., McMahon, G. and Tang, C.** (1999). Design, synthesis, and evaluations of substituted 3-[(3- or 4-carboxyethylpyrrol-2-yl)methylidenyl] indolin-2-ones as inhibitors of VEGF, FGF, and PDGF receptor tyrosine kinases. *J. Med. Chem.* **42**, 5120-5130.

**Valentin, G., Haas, P. and Gilmour, D.** (2007). The chemokine SDF1a coordinates tissue migration through the spatially restricted activation of Cxcr7 and Cxcr4b. *Curr. Biol.* **17**, 1026-1031.

**Venkiteswaran, G., Lewellis, S. W., Wang, J., Reynolds, E., Nicholson, C. and Knaut, H.** (2013). Generation and dynamics of an endogenous, self-generated signaling gradient across a migrating tissue. *Cell* **155**, 674-687.

**Vitorino, P. and Meyer, T.** (2008). Modular control of endothelial sheet migration. *Genes Dev.* **22**, 3268-3281.

**Wilensky, U.** (1999). NetLogo. http://ccl.northwestern.edu/netlogo/. Center for Connected Learning and Computer-Based Modeling, Northwestern University, Evanston, IL USA.

## The model world

Agent-based models were developed initially in Netlogo 4.1, and then subsequently in Netlogo 5.0. To initialize the model, a series of turtles with the identity of either *cxcr4-cell* or *cxcr7-cell* are spawned. Links are established between neighboring turtles (not including diagonal neighbors). Patches along a horizontal stripe on patch wide at the center of the model world begin releasing Cxcl12a at a constant rate (defined by the Cxcl12a-production slider), which diffuses via the Netlogo *diffuse* primitive. The rate and extent of diffusion can be controlled by the Cxcl12a-diffusion-rate and Cxcl12a-diffusion-distance sliders. Diffusion in the model works by removing a fraction (defined by Cxcl12a-diffusion-rate) from the current patch and distributing it equally among all six neighboring patches. This process is repeated *n* number of times (defined by Cxcl12a-diffusion-distance) to produce the final, diffused, pattern.

At each time step, patches provide basal degradation of Cxcl12a, by removing a set percentage of the Cxcl12a from the patch(s) beneath them. This operation is equivalent to the first-order reaction of the form:

$$d[A]/dt = k[A]$$

Where [A] is the Cxcl12a concentration at the patch, and the rate constant *k* is controlled by the Cxcl12a-degredation slider. In the case of degradation by *cxcr4b*- and *cxcr7b-cells*, a similar equation is used, with k controlled by slider determining the rate of degradation by Cxcr4b and Cxcr7b. While degradation by *cxcr7b-cells*, is relatively high, in our model leading *cxcr4-cells* also degrade local Cxcl12a, albeit at a lower rate than *cxcr7-cells*. This degradation by *cxcr4-cells* was essential for leading fragment stretching after severing from trailing cells. To simplify in this case, we assume that the receptors are not limiting for internalization, and do not include a separate term for receptor expression. To model the greater ability of the Cxcr7b protein to internalize and degrade local Cxcl12a, *cxcr7-turtles* also degrade Cxcl12a in all patches which are direct neighbors, and the net degradation rate of these turtles is the sum of the degradation rates assigned to Cxcr4 and Cxcr7.

## Agent behavior in response to Cxcl12a

As we assume that all cells in the PLLp contain some level of Cxcr4b protein, all turtles are competent to respond to Cxcl12a. At each time step, turtles choose a heading randomly within a 120-degree cone around their previous heading and sample the amount of Cxcl12a on the patch ahead of them. Each turtle then determines whether or not it is mechanically restricted from moving by checking whether or not a turtle is present in a 90-degree cone around their current heading. If so, the turtle randomly selects another heading within a 120-degree cone and does nothing further.

If no turtle is present, the agent then calculates whether or not to move in the current heading. In threshold mode, the turtle checks whether the saturating function Cxcl12a / (1 + Cxcl12a) for the patch directly ahead is above the defined threshold. If so, the turtle moves forward a set number of patches (defined by the move variable). If not, the turtle does nothing. In gradient mode, the turtle checks whether the gradient between the current patch and the patch ahead is above a threshold (again, provided by the function Cxcl12a-gradient / (1 + Cxcl12a-gradient). If the gradient is above the gradient threshold, then the turtle moves forward. If not, the turtle does nothing.

After agents have moved, the model recalculates the agent positions based on spring properties of the links that join the agents using the Netlogo *layout-spring* primitive and parameters that can be defined by the user (*spring-constant*, *spring-length* and *repulsion-constant*).

Turtle behavior after cutting

pLLP cutting and rejoining is performed by calculating the links that join turtles at the position defined by the cut-position slider. Links at this position are removed, but the identity of these links (in terms of the turtles they join) is saved. This results in two separate populations of linked cells are subsequently treated independently in the *layout-spring* operation but otherwise operate the same as turtles described above. At each time point a check is performed to see whether turtles from one group are within a minimum range of turtles from the other group (typically within one patch). If this check is passed, the links that were cut are re-established and the agents are reconnected into a single group. Note that to simplify “re-connection”, only one turtle needs to be in range of its previous partner turtle for complete reconnection of all severed links.

For more details on manipulating the model, see the “Info” tab in the model itself.

Click here to Download PLLp model

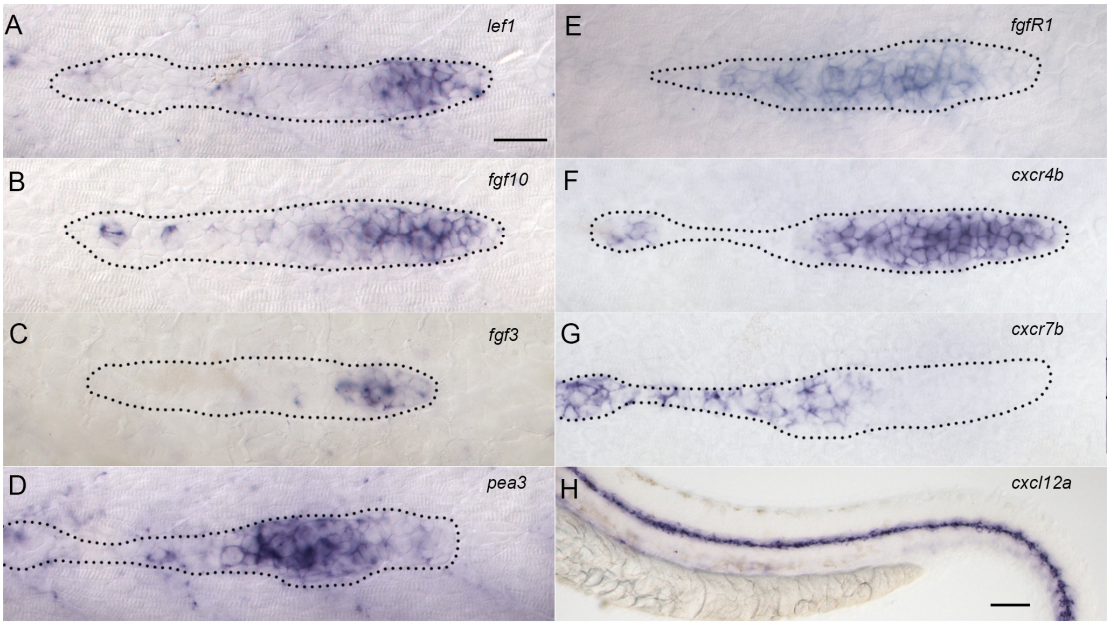


Figure S1
Expression patterns for a selected set of lateral line genes at 32hpf. Scale bar in A-G 10 µm, in H 50 µm.

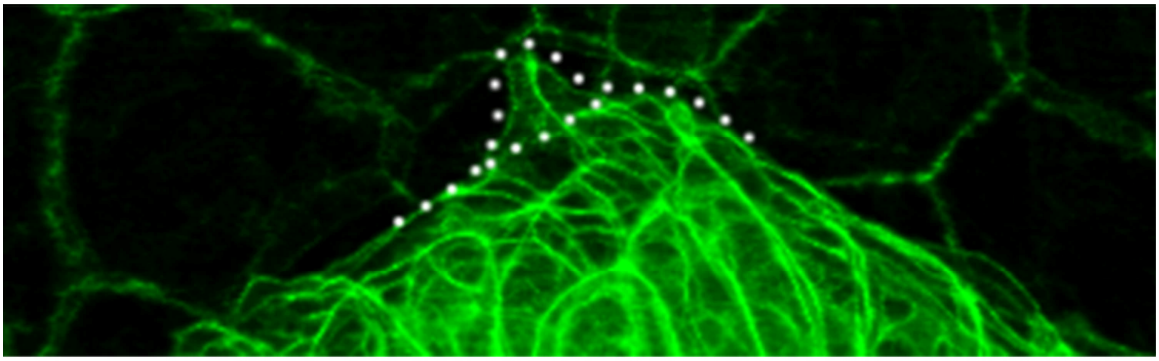

Figure S2: Example of a lateral protrusion from a PLLp after induction of *cxcl12a* expression quantified in figure 2D

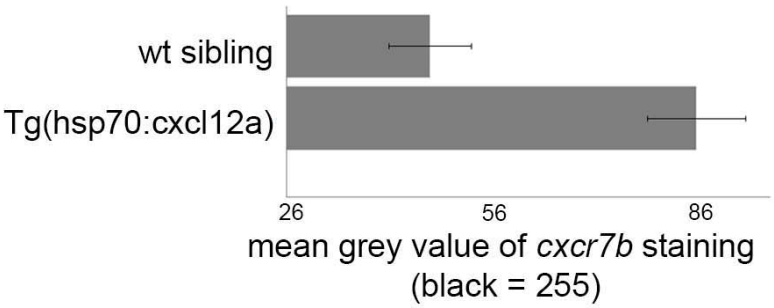


Figure S3: Quantification of mean grey value (+/- st. dev.) for *cxcr7b* staining in *Tg(hsp70:cxcl12a)* and wt sibling embryos 4 hours after heat shock for 30 minutes at 37.5C. Graph is scaled to the average grey value of the *cxcr7b*-free domain of the pLLP (= 26).
$p < 0.001$, Student's two-tailed t-test.

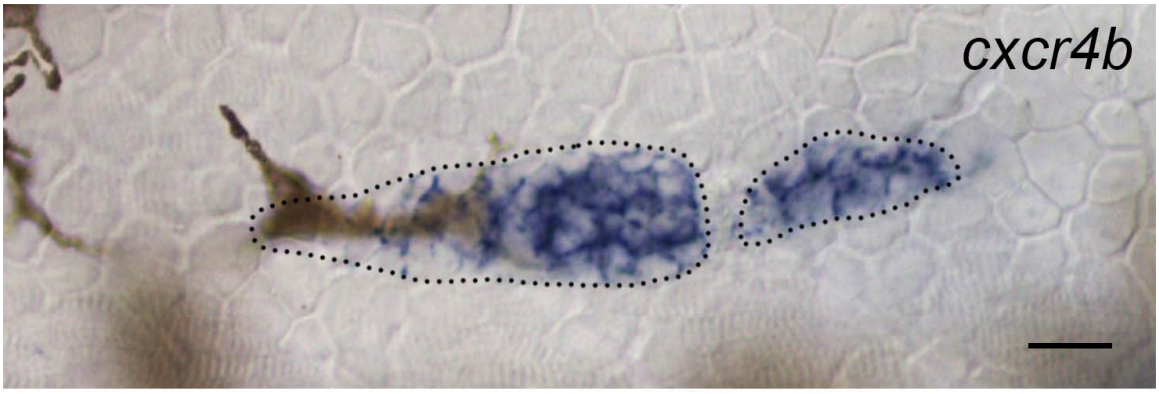


Figure S4
Expression of *cxcr4b* in the PLLp after ablation to sever leading cells. Note that *cxcr4b* is unpolarized in leading cells, while expression remains polarized in trailing cells, as in the unablated PLLp. Scale bar 10 μM.

**Table S1. Embryos examined for each ablation condition.** Summary of number of embryos examined for each experimental condition described in the text.

| Condition | n (embryos) |
|---|---|
| | |
| Basic Ablations | |
| Leading edge severed | 4 |
| Isolated with front and back | 4 |
| Isolated | 13 |
| Isolated with back | 5 |
| Isolated with front | 5 |
| Treated embryos | |
| with SU5402 | 9 |
| With SU5402 washout | 7 |
| With Chalcone-4-Hydrate | 13 |
| Tg(hsp70l:dnfgfr1) | 6 |
| Tg(hsp70l:dnfgfr1) sibling control | 3 |
| Bilateral Bead Transplants | |
| Trailing FGF bead | 6 |
| Leading FGF bead | 6 |
| | |
| Total | 82 |

Table S2: table of pairwise statistical significance of middle fragment centroid movement in various experimental conditions (see Fig. 4N). Students 2-tailed t-test. NS $p > 0.05$

| | | | | | | with SU5402 | hs:dnFGFR1 | hs:dnFGFR1 sibling |
|---|---|---|---|---|---|---|---|---|
| | | X | NS | $p < 0.01$ | $p < 0.001$ | $p < 0.01$ | $p < 0.01$ | NS |
| | | | X | $p < 0.01$ | $p < 0.001$ | $p < 0.05$ | $p < 0.01$ | NS |
| | | | | X | NS | NS | $p < 0.01$ | $p < 0.05$ |
| | | | | | X | $p < 0.05$ | $p < 0.01$ | $p < 0.001$ |
| | with SU5402 | | | | | X | NS | $p < 0.05$ |
| | dnFGFR1 | | | | | | X | NS |
| | dnFGFR1 sibling | | | | | | | X |

**Movie S1**

Time-lapse movie of PLLp in *Tg(hsp:cxcl12a)* embryos after 1 hour heatshock at 37.5°C.


**Movie S2**

Migration of model PLLp (red and green circles) along a stripe of Cxcl12a (blue). Graph indicates Cxcl12a level at the midline. Yellow turtles show active movement, and arrow within turtles indicates direction of movement.

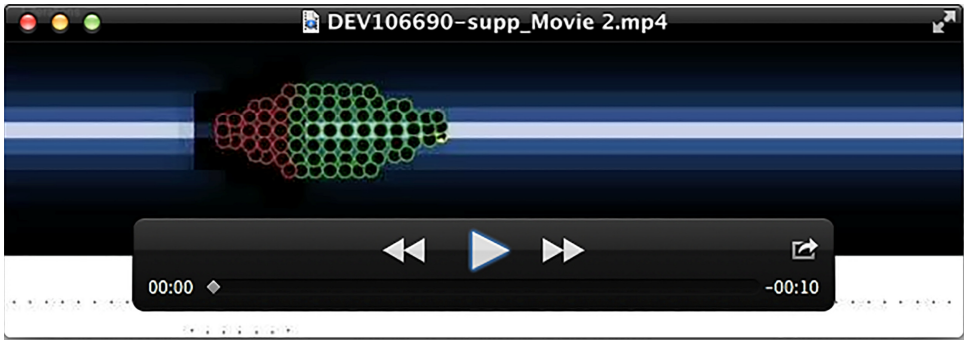

**Movie S3**

Two examples of laser ablation separating a leading fragment from the rest of the PLLp in a *Tg(cldnb:lynEGFP)* embryo. Movie starts at approximately 32hpf. Scale bar = 20µm.

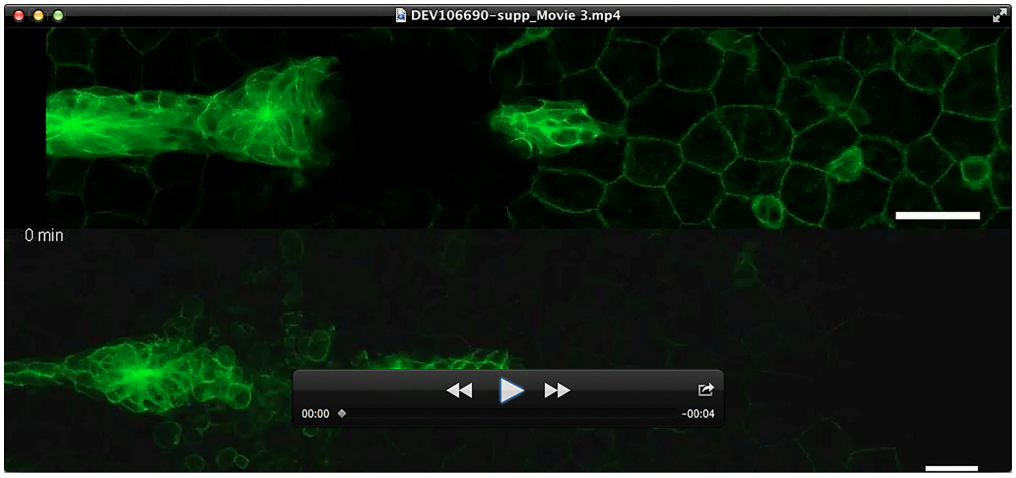


**Movie S4**

Model output when ~20 cells are severed from the tip of the PLLp. Graph indicates Cxcl12a level at midline.

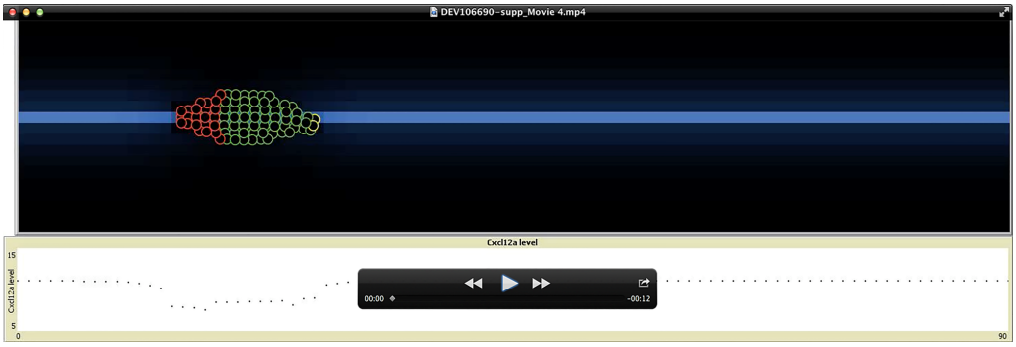

**Movie S5**

Laser ablation separating a leading fragment from the rest of the PLLp in a *Tg(cldnb:lynEGFP)* embryo treated with 10 µM Chalcone-4-Hydrate. Scale bar 10µm.

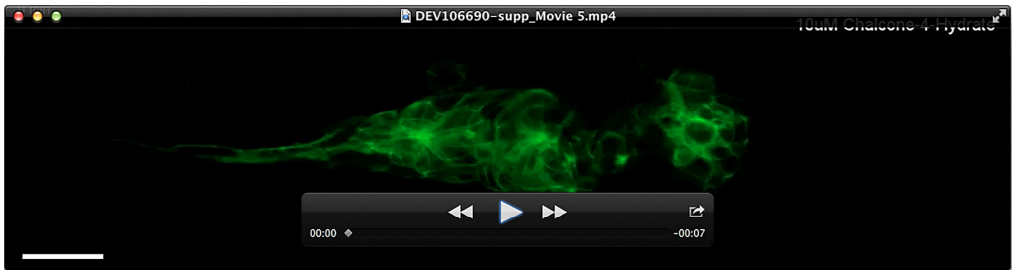


**Movie S6**

Laser ablation to isolate PLLp fragments in *Tg(cldnb:lynEGFP)* embryos. Top panel: Laser ablation of cells surrounding a protoneuromast in a *Tg(cldnb:lynEGFP)* embryo. Second panel: ablation of leading and trailing cells leaving an isolated neuromast. Third panel: ablation mechanically isolating a protoneuromast and ablation of leading cells. Lower panel: ablation mechanically isolating a protoneuromast and ablation of trailing cells. Movies start at approximately 32hpf. Scale bar = 20 µm.

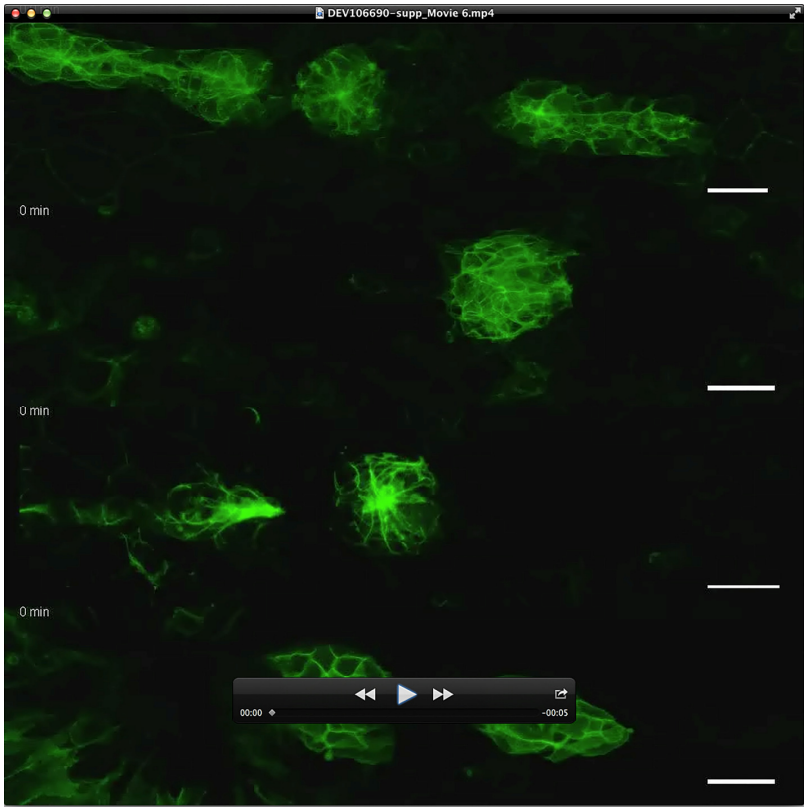

**Movie S7**

Top panel: laser ablation mechanically isolating a protoneuromast and ablation of trailing cells in the presence of 80 µM SU5402 in a *Tg(cldnb:lynEGFP)* embryo. Bottom Panel: laser ablation mechanically isolating a protoneuromast and ablation of trailing cells in the presence of 80µM SU5402 followed by washout of SU5402 with fresh embryo media in a *Tg(cldnb:lynEGFP)* embryo. Movies start at approximately 34hpf. Scale bar = 20 µm.


**Movie S8**

Behavior of an isolated PLLp fragment with beads soaked in recombinant human FGF3 placed either caudally (top panel) or rostrally (bottom panel). BSA soaked beads are transplanted on the opposite side to the FGF3 soaked beads. Scale bar = 20 µm.